# NUMERICALLY EFFICIENT LOW-THRUST FUEL-OPTIMAL COLLISION AVOIDANCE MANEUVERS WITH TANGENTIAL FIRING

**Andrea De Vittori[*], Matteo Omodei[†], Pierluigi Di Lizia[‡], and Roberto Armellin [§]**
**Pau Gago Padreny [¶], Marc Torras Ribell[‖], Jorge Rubio Antón [**], Diego Escobar Antón [††]**

This work presents a numerically efficient fuel-optimal Collision Avoidance Maneuver (CAM) for advanced conjunction notifications with tangential thrusting developed within the Electrocam project in collaboration with ESA and GMV. Given the acceleration profile stemming from the corresponding energy-optimal problem, the algorithm selects candidates firing windows tuned to meet a final constraint in SMD terms for a specified acceleration magnitude. The problem relies on an NLP formulation leveraging only analytic propagators for coasting and thrusting arcs to the advantage of the computational burden. It ensures a good match with the non-linear dynamics attaining competitive fuel mass savings.

## INTRODUCTION

Since the beginning of space exploration, humans have been projecting objects into orbit at an increasing pace. Radars[1] and optical stations regularly watch orbiting objects to update catalogues and predict close encounters providing conjunction data messages to satellite operators. Given that the overcrowding problem is expected to get worse, the chance a typical satellite experiences a possible collision alert during its lifetime is likely to grow. Despite not all alerts requiring evasive action, as the number of alerts increases, it will become impossible to take action from the ground and move to onboard CAM planning is becoming an increasingly topical problem. When designing CAMs, two different models are applicable: the long-term encounter, characterized by non-negligible time spent in the encounter region, and the short-term one, in which the conjunction is almost instantaneous and the assumption of constant relative velocity is valid. To decrease the collision probability, the primary satellite shall perform a maneuver to get away from the secondary object; onboard thrusters

[*]Phd candidate, Department of Aerospace Science and Technology, Politecnico di Milano via Privata Giuseppe La Masa 34, Milano, 20156. Email: andrea.devittori@polimi.it
[†]Graduate student, Department of Aerospace Engineering, Politecnico di Milano, Via Privata Giuseppe La Masa 34, Milano, Lombardia, Italia 20156. Email: matteo.omodei@mail.polimi.it
[‡]Associate professor, Department of Aerospace Science and Technology, Politecnico di Milano via Privata Giuseppe La Masa 34, Milano, 20156. Email: pierluigi.dilizia@polimi.it
[§]Professor, Department of Aerospace Engineering, University of Auckland, 20 Symonds Street, Auckland Central, Auckland, New Zealand 1010. Email: roberto.armellin@auckland.ac.nz
[¶]SSA engineer, GMV, 28760 Tres Cantos, Madrid, Spain. Email: pau.gago.padreny@gmv.com
[‖]Flight dynamics engineer, GMV, 28760 Tres Cantos, Madrid, Spain. Email: marc.torras.ribell@gmv.com
[**]Flight dynamics engineer, GMV, 28760 Tres Cantos, Madrid, Spain. Email: jorge.rubio.anton@gmv.com
[††]Technical Director of SST & STM, GMV, 28760 Tres Cantos, Madrid, Spain. Email: descobar@gmv.com

are used to accomplish this task. Depending on the available acceleration level and the firing time, a maneuver can be classified as impulsive or low-thrust. While the former strategy is achievable with low specific impulse thrusters, low-thrust propulsion maneuvers are typically associated with high specific ones.[2] Among the research studying the impulsive CAM problem, Bombardelli et al. in[3] and[4] formulate an analytical solution to the Optimal Control Problem (OCP) in case of direct and indirect impact. In addition, they provide analytical expressions for the collision kinematics and dynamics of a satellite subject to an impulsive $\Delta v$ in B-plane coordinates.

Conversely, the literature about low-thrust CAMs includes the research of Raiter et al.,[5] who develop a semi-analytical method for just-in-time collision avoidance based on the hypothesis of radial thrust. The solution is obtained by applying a multiple linear regression on the fully numerical solution of the problem, resulting in a polynomial function that, once evaluated, gives the optimal firing time. However, as highlighted by the authors, this approach suffers from stringent validity limits due to the approximations introduced by the multiple linear regression. Besides, Hernando-Ayuso and Bombardelli in[6] develop an analytical solution to the low-thrust CAM design problem by firing with maximum thrust for a fixed time span in the tangential direction to minimize PoC. The result, valid for circular orbits only, serves as the initial guess for the numerical method in which the thrust direction is unconstrained and optimized. Nonetheless, the formulation does not directly consider fuel optimality. Palermo in[7] proposes a fully-analytical formula for the Energy Optimal Control Problem (E-OCP) and a possible solution for the Fuel Optimal Control Problem (F-OCP) with bang-bang acceleration using smoothing techniques and the four-stage Lobatto IIIa formula embedded in the bvp5c MATLAB function. However, the transformation from a continuous acceleration profile to a bang-bang structure cannot always be obtained due to inherent convergence problems of the numeric algorithm when it comes to a highly discontinuous acceleration profile. Furthermore, the recent work by Armellin[8] presents a a multiple-impulse convex formulation for the optimization of low-thrust and impulsive CAMs suitable for autonomous calculations. In the end, the recent work from Pavanello et al.[9] investigated convex optimization to solve trajectory design problems. The method applies the conjunction constraint to the whole window of interest and employs automatic DA dynamics linearization at the expense of computational burden if likened to analytical CAM design. Lastly, D. Shrouti and M. Arun present a study in[1011] that deals with fuel-optimal collision avoidance maneuvers while also incorporating the effects of uncertainty on them. They propose a formulation for convex and another one for non-convex optimization.

This work focuses on a fast semi-analytical method for the design of Advanced Notification fuel-optimal CAMs with tangential control. The approach is built upon the asymptotic solution for the two-body problem with constant tangential thrust acceleration proposed by Bombardelli et al. in[12] and aims at computing the location and duration of a fuel-optimal firing window given a prescribed acceleration magnitude. The pipeline has been developed along with ESA's ELECTROCAM project, funded by ESA and carried out by GMV, Politecnico di Milano and Universidad Carlos III de Madrid. It aims to advance the state-of-the-art in low-thrust collision avoidance activities, focusing on conjunction screening under various sources of uncertainty, such as those arising from the thruster included in uncertainty propagation models detailed by M. Maestrini et al.[13] and.[14] Additionally, the research addresses the design and execution of low-thrust Collision Avoidance Maneuvers (CAMs),[15] taking into account operational constraints to ensure safe and effective decision-making.

## FUNDAMENTALS

This Section summarizes the theoretical principles needed to formulate the aforementioned approaches.

### Conjunction definition

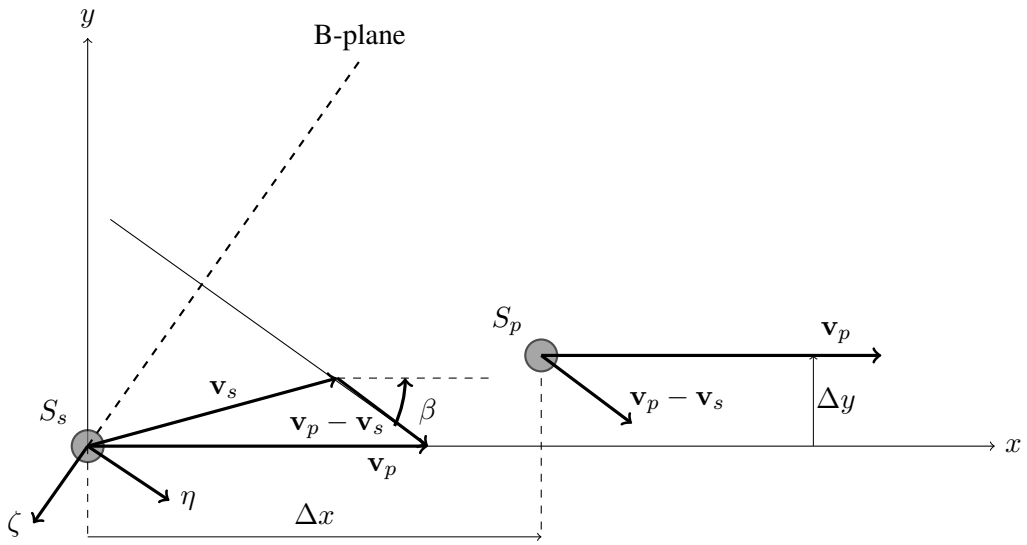


**Figure 1. BPlane representation[16]**

Consider a short-term encounter between a controllable satellite and a debris, hereafter referred to as primary and secondary respectively. The state vectors, position and velocity, of the primary and secondary objects expressed in a generic reference frame (r.f.) $\hat{\Re}$ are defined by $\mathbf{x}_p = [\mathbf{r}_p,\, \mathbf{v}_p]$ and $\mathbf{x}_s = [\mathbf{r}_s,\, \mathbf{v}_s]$. Hence, to compute the collision probability, a more convenient coordinate system is the B-Plane. The latter is centered in the secondary object and is characterized by the following unitary direction vectors:

$$\mathbf{u}_\xi = \frac{\mathbf{v}_p \times \mathbf{v}_s}{||\mathbf{v}_p \times \mathbf{v}_s||},\ \mathbf{u}_\eta = \frac{\mathbf{v}_p - \mathbf{v}_s}{||\mathbf{v}_p - \mathbf{v}_s||},\ \mathbf{u}_\zeta = \mathbf{u}_\xi \times \mathbf{u}_\eta \tag{1}$$

The projection on the $\eta$-axis is given by:

$$\mathbf{R}_{b,2D} = [\mathbf{u}_\xi, \mathbf{u}_\zeta]^\intercal, \tag{2}$$

and the 2D position vector in B-plane r.f. is defined as $\mathbf{b} = [\xi, \zeta]$

### Chan's PoC model

Considering[6] as the main reference, and assuming a Gaussian probability distribution function, the Chan's 2D PoC truncated at the third order $m = 3$ reads:

$$\mathrm{PoC}(u, v) = e^{-\frac{v}{2}} \sum_{m=0}^{3} \frac{v^m}{2^m m!} \left[1 - e^{-\frac{u}{2}} \sum_{k=0}^{m} \frac{u^k}{2^k k!}\right], \tag{3}$$

where $u$ is the ratio of the impact cross-sectional area to the area of the $1\sigma$ B-plane covariance ellipse:

$$u = \frac{s_A^2}{\sigma_\xi \sigma_\zeta \sqrt{1 - \rho_{\xi\zeta}^2}}, \tag{4}$$

and $v$ is the squared Mahalanobis distance (SMD):

$$v = \mathbf{b}_p^\top \mathbf{C}^{-1} \mathbf{b}_p; \tag{5}$$

$\mathbf{C}$ is the covariance matrix, and $\mathbf{b}_p$ is the relative position of primary object with respect to the secondary one in the B-plane r.f..

**Dynamics**

The restricted two-body problem with an acceleration contribution $\mathbf{a}_c$ coupled with the mass equation becomes:

$$\begin{cases} \dot{\mathbf{r}} = \mathbf{v} \\ \dot{\mathbf{v}} = -\dfrac{\mu}{r^3}\mathbf{r} + \mathbf{a}_c \\ \dot{m} = -\dfrac{1}{c_e}\mathbf{a}_c m \end{cases} \quad \text{where : } c_e = I_{sp}\, g_0 \tag{6}$$

**Asymptotic solution of the two-body problem with tangential acceleration**

Bombardelli et al. derived an analytical solution to the two-body problem perturbed by a constant tangential acceleration with the aid of perturbation theory. This section gives just a sneak peek about the topic while the complete and in-depth analysis can be found in.[12]

Coherently with what stated in[17] by Peláez et al., the orbit geometry can be fully described by three generalized orbital parameters assuming that all the acting perturbation forces have a zero component along the normal direction to the orbital plane:[12]

$$q_1 = \frac{e}{h}\cos\Delta\gamma \qquad q_2 = \frac{e}{h}\sin\Delta\gamma \qquad q_3 = \frac{1}{h} \tag{7}$$

where $h$ is the dimensionless angular momentum of the osculating orbit; $e$ is its eccentricity and $\Delta\gamma$ is, for this particular case in which the orbit plane is constant, the rotation of the eccentricity vector with respect to the initial orbit. The evolution of the three generalized orbital parameters in case of purely tangential acceleration is:

$$\frac{d}{d\theta}\begin{bmatrix} q_1 \\ q_2 \\ q_3 \end{bmatrix} = \frac{\epsilon}{q_3 s^3 \sqrt{e^2 + 2e\cos\nu + 1}} \begin{bmatrix} s\sin\theta & (s+q_3)\cos\theta \\ -s\cos\theta & (s+q_3)\sin\theta \\ 0 & -q_3 \end{bmatrix} \begin{bmatrix} e\sin\nu \\ 1 + e\cos\nu \end{bmatrix}, \tag{8}$$

where $\theta$ is the independent variable used in the Peláez method and is equal to:

$$\theta = \nu + \Delta\gamma, \tag{9}$$

$\nu$ is the true anomaly of the osculating orbit; $s$ is the dimensionless transverse velocity of the object

$$s = q_1\cos\theta + q_2\sin\theta + q_3, \tag{10}$$

and $\epsilon$ is the corresponding dimensionless value of the constant tangential acceleration $A_t$:

$$\epsilon = \frac{A_t}{\mu/r_0^2}. \tag{11}$$

When considering small perturbations ($\epsilon \ll 1$), the three generalized orbital parameters can be written as power series through an asymptotic expansion of Eq. 8:

$$\begin{cases} q_1(\theta,\epsilon) = q_{10} + \epsilon q_{11}(\theta) + o(\epsilon) \\ q_2(\theta,\epsilon) = q_{20} + \epsilon q_{21}(\theta) + o(\epsilon) \\ q_3(\theta,\epsilon) = q_{30} + \epsilon q_{31}(\theta) + o(\epsilon) \end{cases}, \tag{12}$$

where the zeroth order terms are the constant generalized orbital elements of the unperturbed trajectory:

$$q_{10} = \frac{e_0}{h_0} \qquad q_{20} = 0 \qquad q_{30} = \frac{1}{h_0} \ , \tag{13}$$

and the first order terms expressed as a function of a new variable $\tilde{E}$ are:

$$\begin{cases} q_{11}(\tilde{E},h_0,e_0) = \frac{h_0^3}{\left(1-e_0^2\right)^2}\left[Q_{11}(\tilde{E},e_0) - Q_{11}(\tilde{E}_0,e_0)\right] \\ q_{11}(\tilde{E},h_0,e_0) = \frac{h_0^3}{\left(1-e_0^2\right)^{\frac{3}{2}}}\left[Q_{21}(\tilde{E},e_0) - Q_{21}(\tilde{E}_0,e_0)\right] \\ q_{31}(\tilde{E},h_0,e_0) = \frac{h_0^3}{\left(1-e_0^2\right)^2}\left[Q_{31}(\tilde{E},e_0) - Q_{31}(\tilde{E}_0,e_0)\right] \end{cases}, \tag{14}$$

being $\tilde{E}$ equal to:

$$\tan\frac{\tilde{E}}{2} = \sqrt{\frac{1-e_0}{1+e_0}}\tan\frac{\theta}{2}. \tag{15}$$

The complete description of the solution and the analytical expression of the $Q_{i,1}(e_0,\tilde{E})$ functions are available in.[12]

However, the evolution of the generalized orbital parameters has been obtained relying on the variables $\tilde{E}$ or equivalently $\theta$. To infer the orbit characteristics at any desired epoch, it is necessary to express $q_1$, $q_2$ and $q_3$ as a function of time. To this end, the series expansion of the time can be conveniently written as:

$$t(\epsilon,\tilde{E}) = t_0(\tilde{E}) + \epsilon t_1(\tilde{E}) + o(\epsilon), \tag{16}$$

where $t_0(\tilde{E})$ corresponds to the time of the unperturbed trajectory

$$t_0(e_0,\tilde{E}) = \frac{h_0^3}{\left(1-e_0^2\right)^{\frac{3}{2}}}\left[T_{kep}(\tilde{E}) - T_{kep}(\tilde{E}_0)\right], \tag{17}$$

with

$$T_{kep} = \tilde{E} - e_0\sin\tilde{E}, \tag{18}$$

while the first order term is:

$$t_1(e_0,\tilde{E}) = \frac{h_0^7}{\left(1-e_0^2\right)^{\frac{9}{2}}}\left[T(\tilde{E}) - T(\tilde{E}_0)\right], \tag{19}$$

with the analytical expression of $T(\tilde{E})$ available in.[12]

## ADVANCED NOTIFICATION CAM WITH TANGENTIAL CONTROL

Energy-optimal (EO) CAMs are widely used in the literature for maneuver optimization. That said, they output a continuously varying unbounded acceleration that may exceed the thruster capabilities. Bang-bang control profiles with a fixed acceleration level can solve this issue by shaping the propulsion system functioning in an operative scenario and satisfying conditions on the desired PoC. Fortunately, the EO solution, by looking at the maxima of the continuous acceleration norm, gives a hint for candidate optimal bang-bang windows placement. In this context,[7] shows that tangential maneuvers almost align with the free directional CAM for advanced conjunction notification.

This section is devoted to describing the Fuel-Optimal CAM with tangential firing as a two-step process. It requires an acceleration profile guess stemming from the corresponding EO formulation and tunes the firing windows with an NLP optimization problem.

### Energy-optimal CAM with tangential thrust

The analytical CAM formulation for short-term encounters formulates as two-boundary value problem with the following control acceleration:

$$\mathbf{a}_c = a_{\max}\epsilon\mathbf{t}, \quad \text{where} \quad \mathbf{t} = \frac{\mathbf{v}}{v}. \tag{20}$$

$a_{\max}$ is the maximum acceleration. The Euler-Lagrange equations describing the problem are:

$$\begin{cases} \dot{\mathbf{r}} = \mathbf{v} \\ \dot{\mathbf{v}} = -\dfrac{\mu}{r^3}\mathbf{r} - a_{\max}\left(\boldsymbol{\lambda}_v \cdot \dfrac{\mathbf{v}}{v}\right)\dfrac{\mathbf{v}}{v} \\ \dot{\boldsymbol{\lambda}}_r = \dfrac{\mu}{r^3}\boldsymbol{\lambda}_v - \dfrac{3\mu\mathbf{r}\cdot\boldsymbol{\lambda}_v}{r^5}\mathbf{r} \\ \dot{\boldsymbol{\lambda}}_v = -\boldsymbol{\lambda}_r + a_{\max}\left( - \left(\dfrac{\boldsymbol{\lambda}_v \cdot \mathbf{v}}{v^2}\right)^2 \mathbf{v} + \dfrac{\boldsymbol{\lambda}_v \cdot \mathbf{v}}{v^2}\boldsymbol{\lambda}_v \right) \end{cases} \tag{21}$$

With the following boundary conditions:

$$\begin{cases} \mathbf{r}(t_0) = \mathbf{r}_0 \\ \mathbf{v}(t_0) = \mathbf{v}_0 \\ \boldsymbol{\lambda}_r(t_f) = \nu\dfrac{\partial d_M^2(\mathbf{r}_f)}{\partial \mathbf{r}_f} = 2\nu\mathbf{R}_{2\mathrm{D}}^{\top}\mathbf{C}^{-1}\mathbf{R}_{2\mathrm{D}}(\mathbf{r}_f - \mathbf{r}_s) \\ \boldsymbol{\lambda}_v(t_f) = \nu\dfrac{\partial d^2(\mathbf{v}_f)}{\partial \mathbf{v}_f} = \mathbf{0} \\ d_M^2(\mathbf{r}_f) - \bar{d}_M^2 = 0. \end{cases} \tag{22}$$

From this point on, the analytical and computationally efficient CAM derivation can be found in Sect. 3 of.[7] The initial costates are found through motion linearization and the integration of the equations of motion outputs the acceleration profile magnitude $a_{EO}^{tan}$.

### Fuel-Optimal CAM with tangential thrust

This section addresses the semi-analytical solution of the TPBVP with prescribed acceleration $a_{max}$ and unknown firing windows. The solution process starts with the identification of the nominal

firing windows from the tangential EO problem. The latter is here exploited to get a first guess on the optimal firing windows. The equivalent burning time $t_b$ is estimated using the acceleration $a_{EO}^{tan}(t)$ resulting from the tangential EO with continuous thrust.

$$t_b = \frac{\Delta v}{a_{max}} = \frac{1}{a_{max}} \int_{t_0}^{t_f} a_{EO}^{tan}(t)\ dt \tag{23}$$

Then, the idea is to define $a_{c,th}$ so that the thrusters are fired for $a_{EO}^{tan} \geq a_{th}$ and switched off otherwise. To this purpose, once $a_{max}$ is set, a bisection method is used to retrieve $a_{th}$. The procedure is described below:

1. Set two initial boundary values for $a_{th}$ for the first bisection iteration, namely $a_{th_1} = \max(a_{EO}^{tan})$ and $a_{th_2} = \min(a_{EO}^{tan})$;
2. Evaluate the burning time $t_b^c$ for $a_{EO}^{tan} \geq a_{th_1}$ and for $a_{EO}^{tan} \geq a_{c,th_2}$;
3. Iteratively update $a_{th_1}$ or $a_{th_2}$ with the bisection method taking as cost function $J = t_b^c - t_b$;
4. Do step 3 until $|t_b^c - t_b| \leq \Delta t$ with $\Delta t$ a prescribed tolerance.

Figure 2 shows the end result stemming from the reported bisection method

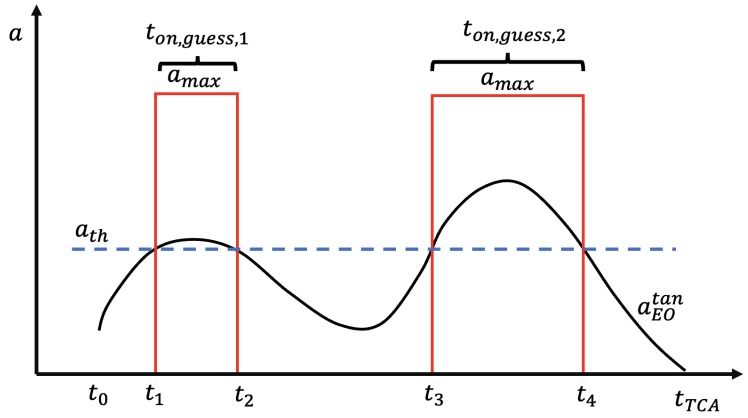


**Figure 2. Bisection method representation to find candidate firing windows given $a_{EO}^{tan}$.**

Within the Electrocam project, it is required to simulate only a single firing window to comply with GMV's operative constraints. The algorithm tests separately the guessed windows found through the bisection method, and it chooses the one featuring the lowest $\Delta v$ figure. The FO CAM solves adopting a NLP approach (Non-Linear Programming) approach, stated as follows:

$$J = d_M^2\left(\boldsymbol{r_{p,f}}(\boldsymbol{t_{on,i}}), \boldsymbol{r_{s,f}}\right) - \bar{d_M^2} \tag{24}$$

$\boldsymbol{t_{on,i}} = \boldsymbol{\gamma_i} \cdot \boldsymbol{t_{on,guess,i}}$ is the i-th firing windows stemming from the enlarged or shortened guess counterpart ($\boldsymbol{t_{on,guess,i}}$) visible in Fig.2. $\boldsymbol{\gamma_i}$ is the actual minimization variable constrained to $\boldsymbol{\gamma_i} \geq 0$. $d_M^2\left(\boldsymbol{r_{p,f}}(\boldsymbol{t_{on,i}}), \boldsymbol{r_{s,f}}\right) - \bar{d_M^2}$ stands for the difference between the current SMD and the target one. It depends on the secondary position $\boldsymbol{r_{s,f}}$ and primary $\boldsymbol{r_{p,f}}$ at TCA. After the

optimization procedure, the tuned firing windows and the Bplane position will look like the ones shown in Fig. 3, where the first thrust arc appears to be the most efficient fuel-wise.

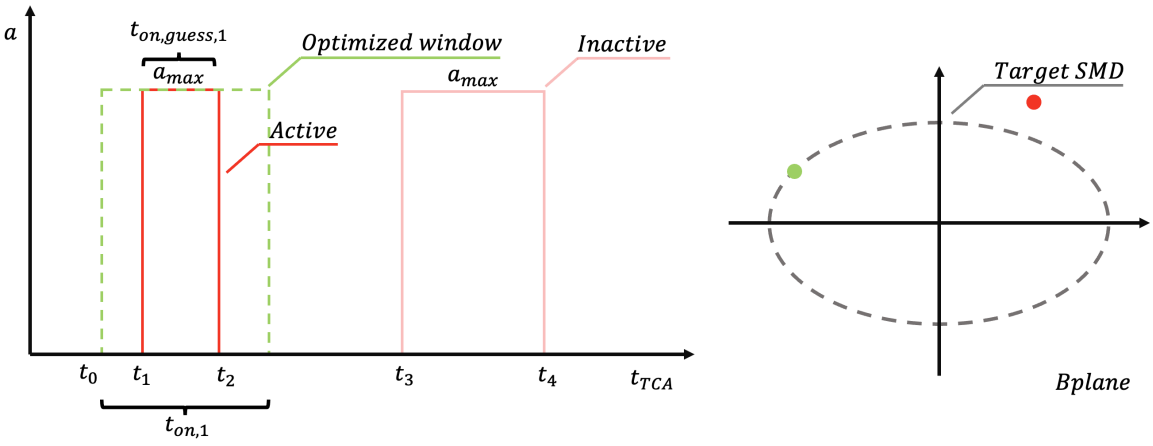


**Figure 3. Optimal magnitude acceleration profile on the left and the corresponding Bplane on the right.**

Up to this stage, the nominal firing windows have been sought in the time domain. However, in the Bombardelli derivation, the evolution of the generalized orbital parameters $(q_1, q_2, q_3)$ is not a function of time but rather of the $\tilde{E}$ parameter (or equivalently $\theta$). Hence, the nominal on-off time windows obtained thanks to the bisection method shall be transformed into equivalent true anomaly ranges $\boldsymbol{\theta_{span}}$, as follows with an example:

$$\boldsymbol{\theta_{span}} = [\overbrace{\theta_0, \theta_1}^{off}, \underbrace{\theta_1, \theta_2}_{on}, \overbrace{\theta_2, \theta_{tca}}^{off}] \quad if \quad \boldsymbol{t_{on,guess,i} = t_{on,guess,1}} \tag{25}$$

The same transformation holds for the firing durations:

$$\boldsymbol{t_{on,i} = \gamma_i \cdot t_{on,guess,i} \rightarrow \Delta\theta_{on,i} = \alpha_i \cdot \Delta\theta_{on,guess,i}} \tag{26}$$

all $\boldsymbol{\alpha_i} = 1$ for the variable initialization. The orbital parameters of the primary body change during the accelerated dynamics, so they are updated in the analytical propagation to avoid undesired shifts (see Alg. 1).The EO solution comes in handy also to understand if the spacecraft acceleration is more tangential or anti-tangential for each bang. Therefore, a vector of maximum accelerations $\boldsymbol{a_{max}}$ is defined as follows:

$$\boldsymbol{a_{max}} = [a_{max,1}, ..., a_{max,N}] \tag{27}$$

Such that:

$$\begin{cases} a_{max,i} = a_{max} \; if \; \boldsymbol{a_{EO}^{tan}}(t) = k\boldsymbol{t} \; with \; k > 0 \; in \; \boldsymbol{t_{on,guess,i}} \\ a_{max,i} = -a_{max} \; if \; \boldsymbol{a_{EO}^{tan}}(t) = -k\boldsymbol{t} \; with \; k > 0 \; in \; \boldsymbol{t_{on,guess,i}} \end{cases} \tag{28}$$

Fig. 4 gives a wrap-up of all the steps described within the pipeline for FO CAM. In the context of the Electrocam project, the solutions of FO CAMs are fed to advanced CAM optimization tools

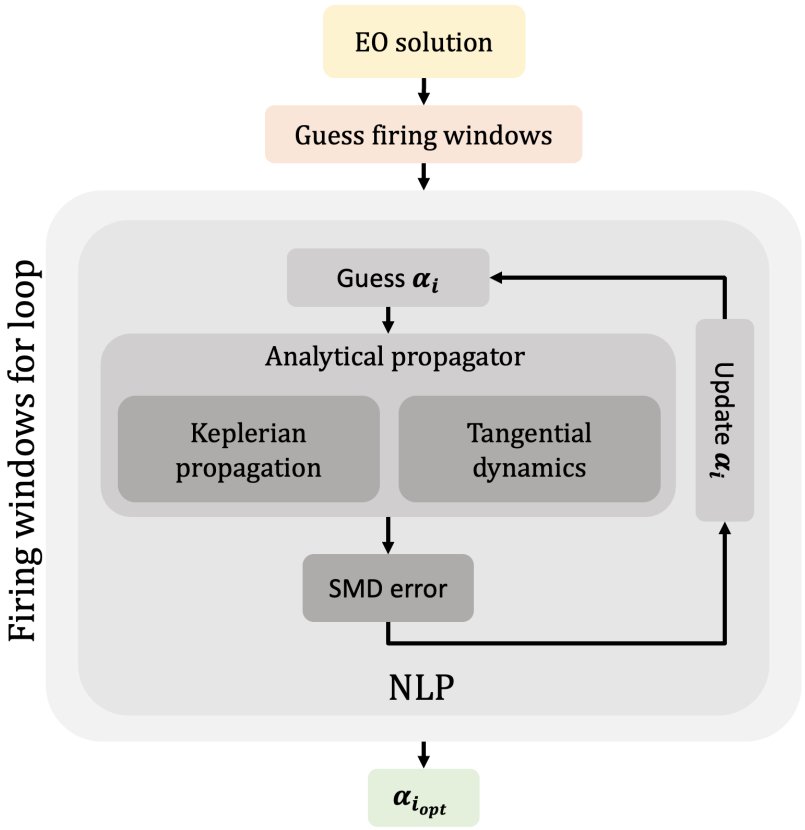


**Figure 4. Pipeline wrap-up for the firing windows computation**

developed by GMV that encompass perturbations and operative constraints. As previously stated, among all $i-th$ candidate windows, the one having the minimum firing time is taken as the final solution.

**Algorithm 1** Propagation core

**Input:**
$\boldsymbol{\alpha_i}$: Firing window multiplier
$\boldsymbol{x_{p0}}$: Primary mean state at $t_0$
$\mu$: Gravitational constant
$\boldsymbol{\Delta\theta_{on,guess,i}}$: True anomaly interval guess for tangential firing
$\boldsymbol{\theta_{span}}$: Vector containing true anomaly guess windows for ballistic and accelerated dynamics
$\boldsymbol{a_{max_i}}$: tangential or anti-tangential maximum acceleration
$t_{tca}$: Time of closest approach
$d_M^2$: Target SMD
$\boldsymbol{r_{s,f}}$: Position of the secondary at TCA
**Output:**
$t_{on}$: Firing time
$d_{M,err}^2$: SMD error
**Analytical Propagation:**
$\boldsymbol{kep_0} = car2kep(\boldsymbol{x_{p0}}, \mu)$: From cartesian to keplerian elements
$t_{on+off} = 0$ Total propagation time initialization
$lim = length(\boldsymbol{\theta_{on,guess,i}})$ (dimension 1); $k = 0$ counter for on windows initialization
**for** the index $n = 1 : 2 : length(\boldsymbol{\theta_{span}})$ **do**
  **if** the thrusters in $\boldsymbol{\theta_{span}}(n, n+1)$ are on **then**
    $[\boldsymbol{x_{p,prop}}, t_{prop,on}] = Bombardelli_{propagator}(\boldsymbol{x_{p0}}, \boldsymbol{\alpha_i \Delta\theta_{on,guess,i}}, \boldsymbol{a_{max,i}}, \mu)$
    $\boldsymbol{x_{p,0}} = \boldsymbol{x_{p,prop}}$ Update the initial state
    $t_{prop,on+off} = t_{prop,on+off} + t_{prop,on}$ Update the propagation time
    k=k+1
  **else if** the thrusters in $\boldsymbol{\theta_{span}}(n, n+1)$ are off **then**
    $\boldsymbol{kep}_0 = car2kep(\boldsymbol{x_{p,0}}, \mu)$ Update the keplerian elements
    **if** $k < lim$ **then**
      **if** $\boldsymbol{\theta_{span}}(n+2, n+3) \neq \boldsymbol{\theta_{span}}(end-1, end)$ **then**
        $t_{prop,off} = \Delta\theta 2\Delta\mathrm{t}(\boldsymbol{kep}_0, \boldsymbol{\theta_{span}}(n+1) - 0.5 \cdot (\boldsymbol{\alpha_i} - 1)\boldsymbol{\Delta\theta_{on,guess,i}}, \mu)$ Equivalent Keplerian $\Delta$t
      **else**
        $t_{prop,off} = \Delta\theta 2\Delta\mathrm{t}(\boldsymbol{kep_0}, \boldsymbol{\theta_{span}}(n+1) - (\boldsymbol{\alpha_i} - 1)\boldsymbol{\Delta\theta_{on,guess,i}}, a_{max,i}, \mu)$ Equivalent Keplerian $\Delta$t
      **end if**
      $t_{prop,on+off} = t_{prop,on+off} + t_{prop,off}$ Update the propagation time
    **else**
      $t_{prop,off} = t_{TCA} - t_{prop,on+off}$ Equivalent Keplerian $\Delta$t
    **end if**
    $\boldsymbol{\Delta\theta}_{prop,off} = \Delta\mathrm{t}2\Delta\theta(\boldsymbol{kep_0}, t_{prop,off}, \mu)$ Equivalent Keplerian $\Delta\theta$
    $\boldsymbol{x_{p,prop}}$= kep2car$_{propagator}(\boldsymbol{kep_0}, \boldsymbol{\Delta\theta}_{prop,off}, \mu)$
    $\boldsymbol{x_{p,0}} = \boldsymbol{x_{p,prop}}$ Update the initial state
  **end if**
**end for**
$\boldsymbol{r_{p,f}} = \boldsymbol{x_{p,0}}(1:3)$ primary position state at TCA
$d_{M,err}^2 = d_M^2(\boldsymbol{r_{p,f}}, \boldsymbol{r_{s,f}}) - \bar{d_M^2}$

## RESULTS

### Test Cases description

To prove the algorithm's effectiveness, it is tested against a set of seven Conjunction Data Messages (CDMs) ranging from low to geostationary orbits. The dataset has been kindly provided by GMV during the Electrocam project.The Primaries orbit representation is displayed in Fig. 5, whilst the secondaries counterpart are detailed in Fig. 6. For sake of conciseness, only the encounter data of LEOH2HMD is shown in Tab. 1.

**Table 1. LEOH2HMD test case conjunction data.**

| | |
|---|---|
| $\mathbf{r}_p$[km] | [-5113.9219 , 27.0979 , 5545.0427 ]$^\top$ |
| $\mathbf{r}_s$[km] | [-5113.9225 , 27.0498 , 5545.0444 ]$^\top$ |
| $\mathbf{v}_p$ [km/s] | [-5.3416 , -0.3599 , -4.9236 ]$^\top$ |
| $\mathbf{v}_s$ [km/s] | [7.3537, -1.1428, -0.19825]$^\top$ |
| PoC | 0.0271 (Chan) |
| $d$ [m] | 48.131 |

The corresponding covariance matrix for the primary and secondary in ECI and plane coordinates is:

$$\mathbf{C}_p = \begin{bmatrix} 1.6602 & -1.1612 & -0.14638 \\ -1.1613 & 233.6017 & 0.0228 \\ -0.1464 & 0.0228 & 2.9134 \end{bmatrix} \cdot 10^{-4}\ \mathrm{km}^2 \tag{29}$$

$$\mathbf{C}_s = \begin{bmatrix} 1.5805 & -3.1446 & 0.0023 \\ -3.1446 & 251.6288 & -0.1267 \\ 0.0023 & -0.1267 & 1.0296 \end{bmatrix} \cdot 10^{-4}\ \mathrm{km}^2 \tag{30}$$

Projecting the summed covariances in the Bplane frame results in

$$\mathbf{C} = \begin{bmatrix} 3.1792 & -0.1191 \\ -0.1191 & 4.5824 \end{bmatrix} \cdot 10^{-4}\ \mathrm{km}^2 \tag{31}$$

The objects combined cross-sectional radius $s_A = 15\ m$ , and the operative satellites features a propulsion system granting a constant acceleration $a_{max} = 0.1\frac{mm}{s^2}$. To reduce the collision likelihood, it targets a collision probability $PoC = 10^{-6}$, a typical value applied to operative scenarios. In all the encounters, to see how effective is acting in advance, the primary performs CAMs on 31 equally space initial maneuvering points from 0.5 to 8 orbits before TCA. All the simulations conducted for this work are run on an Intel(R) Core(TM) i7-10700 CPU processor with 16 GB of Ram Memory.

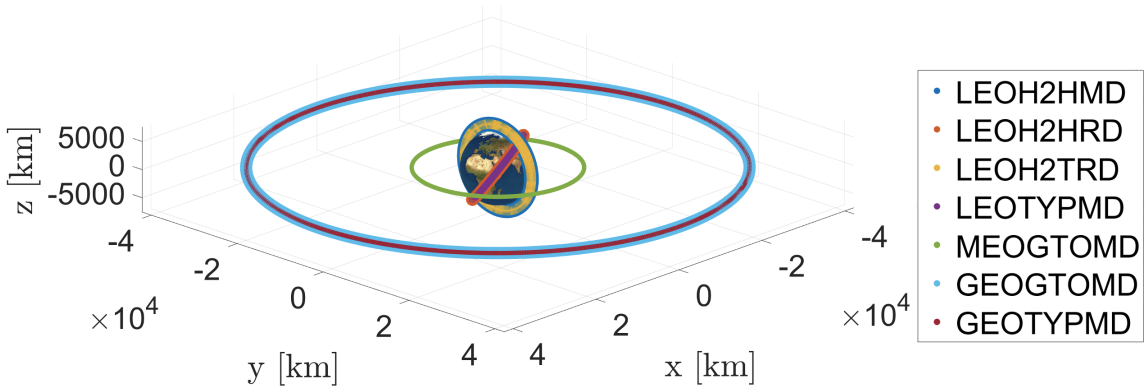


**Figure 5. Primaries ballistic trajectory representation in ECI frame**

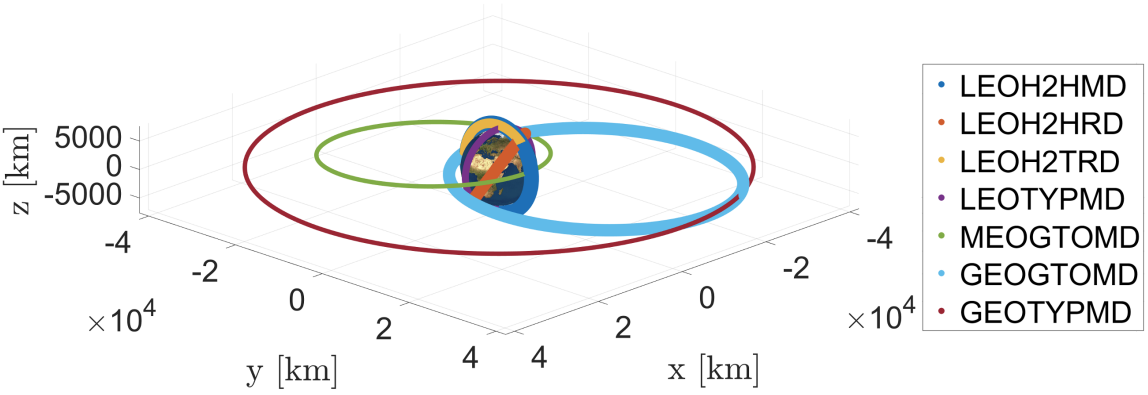


**Figure 6. Secondaries ballistic trajectory representation in ECI frame**

### Energy-Optimal CAM with tangential thrust

In accordance with the proposed solution flow, the first analysed algorithm is the EO CAM with Chan's PoC boundary constraint. Especially, Fig. 7 displays the collision probability for CAMs with a tangential firing after a numerical integration of the dynamics with the solution provided by the motion linearization. In all scenarios, there is a good agreement between the enforced PoC value and the resulting one after a numerical integration with few exceptions: LEOH2HRD experience a deviation of one order of magnitude with regard to the reference PoC. Notwithstanding, the EO solution serves just as a guess for a more applicable fuel-optimal policy.

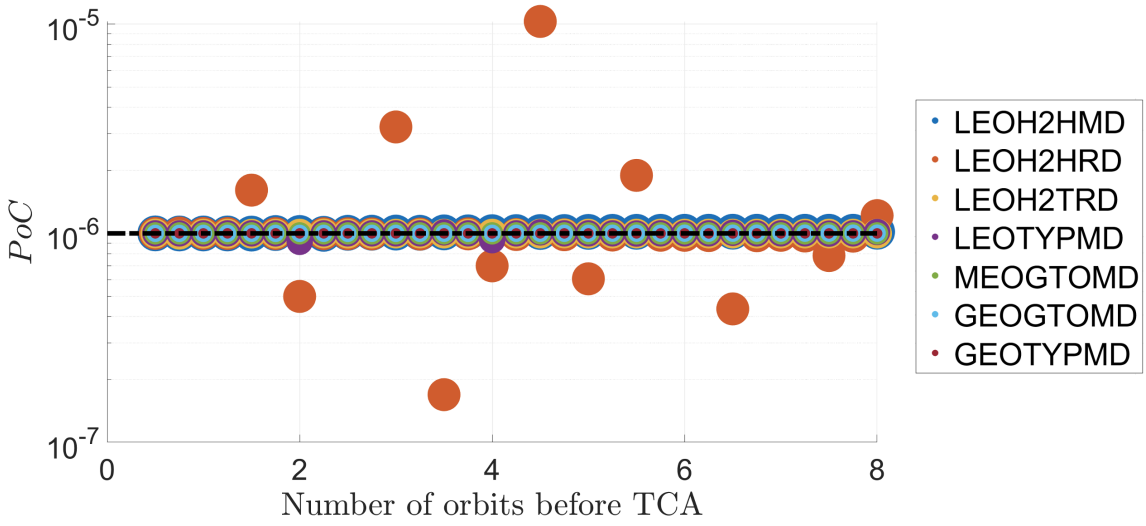


**Figure 7. Collision probability for the EO CAM. The initial maneuvering points go from 0.5 to 8 before TCA.**

Pertaining to the $\Delta v$ manoeuvre cost in Fig. 8, it appears evident that designing CAMs beforehand saves fuel with a decreasing trend even at 8 orbits before TCA. This figure of merit is worth comparing with the FO counterpart presented in the section below (Fig. 10).

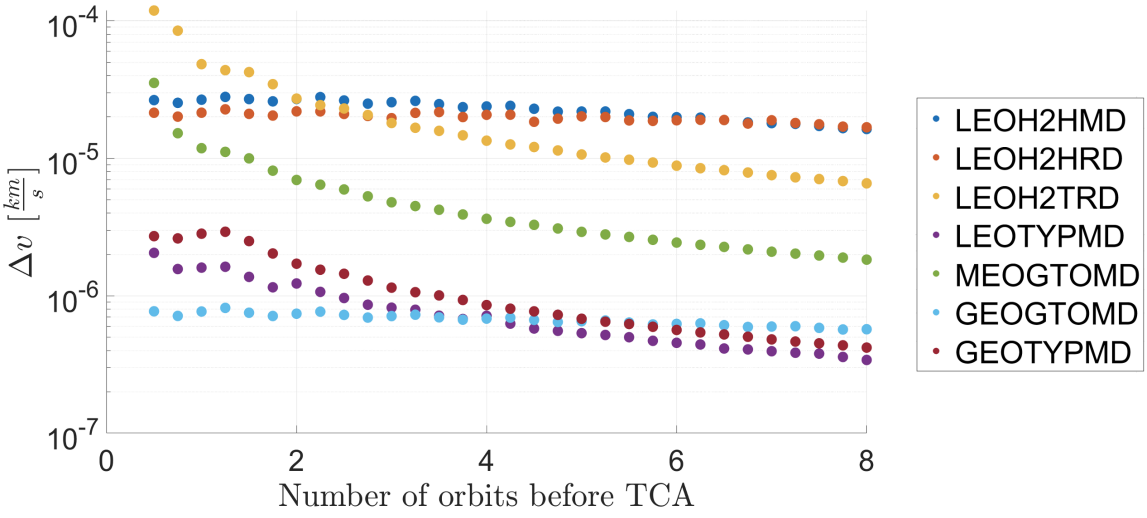


**Figure 8. $\Delta v$ cost for the EO CAM. The initial maneuvering points go from 0.5 to 8 before TCA.**

### Fuel-Optimal CAM with tangential thrust

Moving on to FO CAMs, after a numerical integration for results validity, PoC assessment shows that no accuracy concern occurs other than to the LEOH2TRD case when thrusting tangentially close to conjunction. That said, the error is still within one order of magnitude if likened to $10^{-6}$.

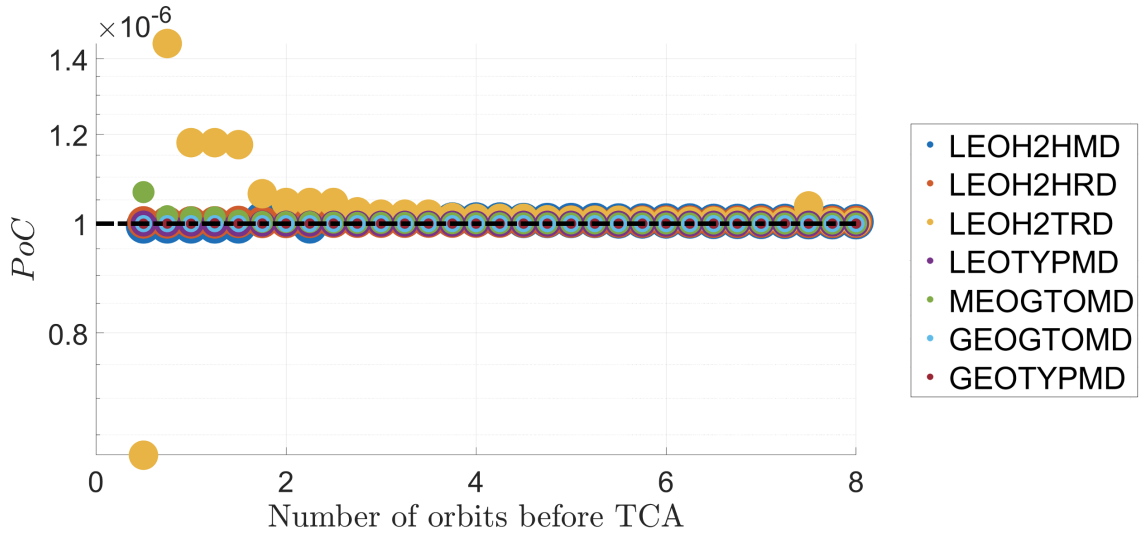


**Figure 9. Collision probability for the FO CAM. The initial maneuvering points go from 0.5 to 8 before TCA.**

$\Delta$v follows the same pattern as the EO solution, saving even more fuel with the FO strategy, as seen in Fig. 10. Notably, in some combinations of initial maneuvering point/scenario $\Delta v$ is down by two or three times.

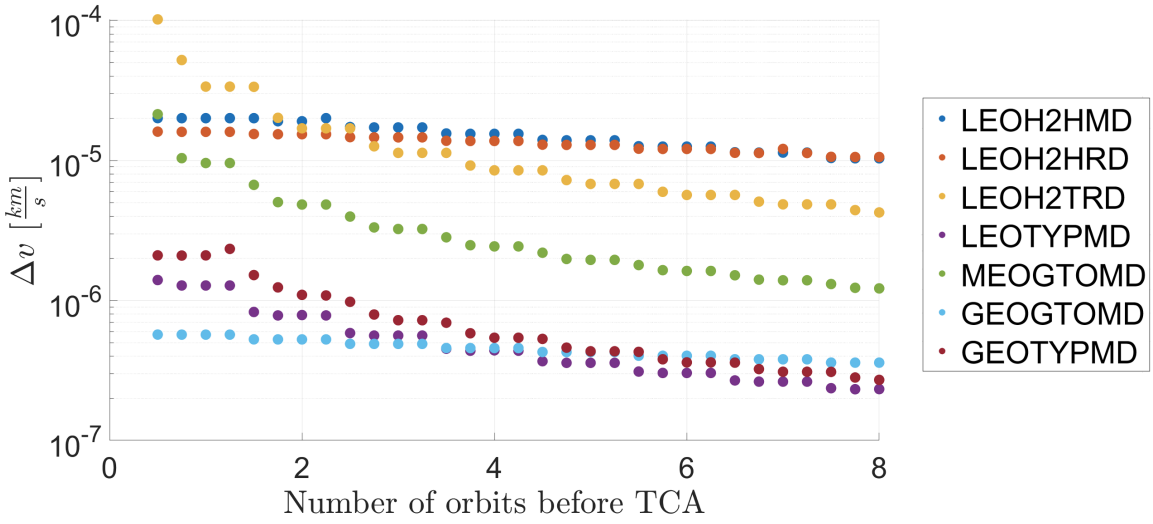


**Figure 10. $\Delta v$ cost for the FO CAM. The initial maneuvering points go from 0.5 to 8 before TCA.**

Fig. 11 reports the bang-bang acceleration profile typical of a FO approach close to conjunction. The orange line links to the EO tangential CAM and the black one to the FO policy. Given that $a_{max}$ is approximately one order of magnitude higher than the maximum EO acceleration norm, the engine are on for roughly 150 s. If compared to traditional continuation techniques, the presented

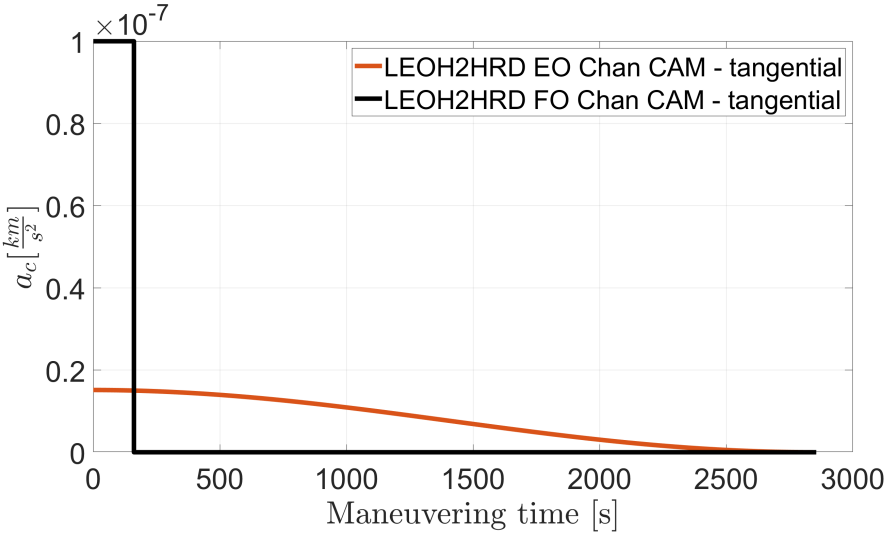


**Figure 11. Acceleration profile for a relatively short notification maneuver**

pipeline is not influenced by steep thrust variations and short firings. Noteworthy, if the EO CAM is lagging behind too much, the FO strategy may not cope with it. Planning CAMs in advance makes the EO solution experience lower acceleration levels as seen in Fig. 12, limiting fuel expenditure. Nonetheless, satellite operators have to take into account additional constraints: Earth's shadowing, objects' uncertainty evolution, and communication shutdowns.

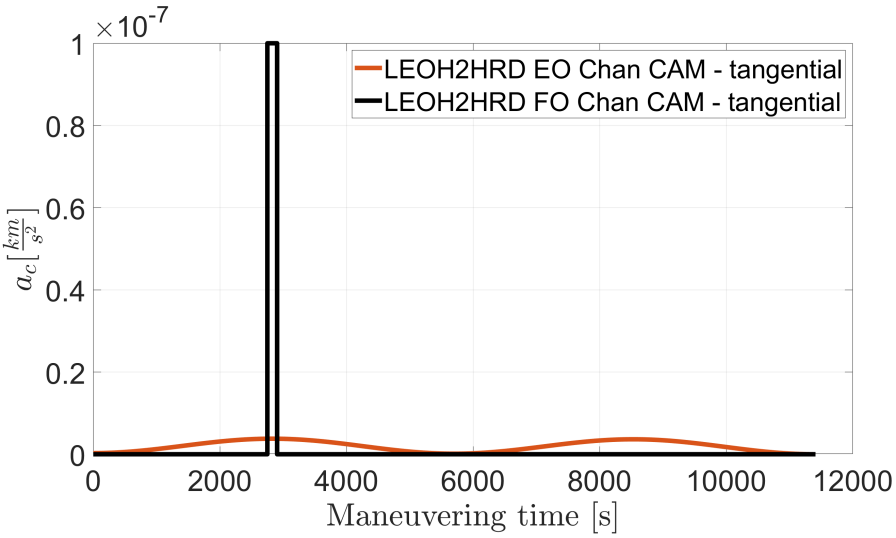


**Figure 12. Acceleration profile for a long notification maneuver**

Lastly, an equivalent Bplane depicts the maneuver effect at conjunction in Fig. 13. The rhomboidal markers are tied to the primary following a ballistic trajectory. Dots refer to the EO CAM while triangles to the FO equivalent. The EO and FO procedure make the primary land on an iso-probability ellipse as expected by Chan's PoC model.

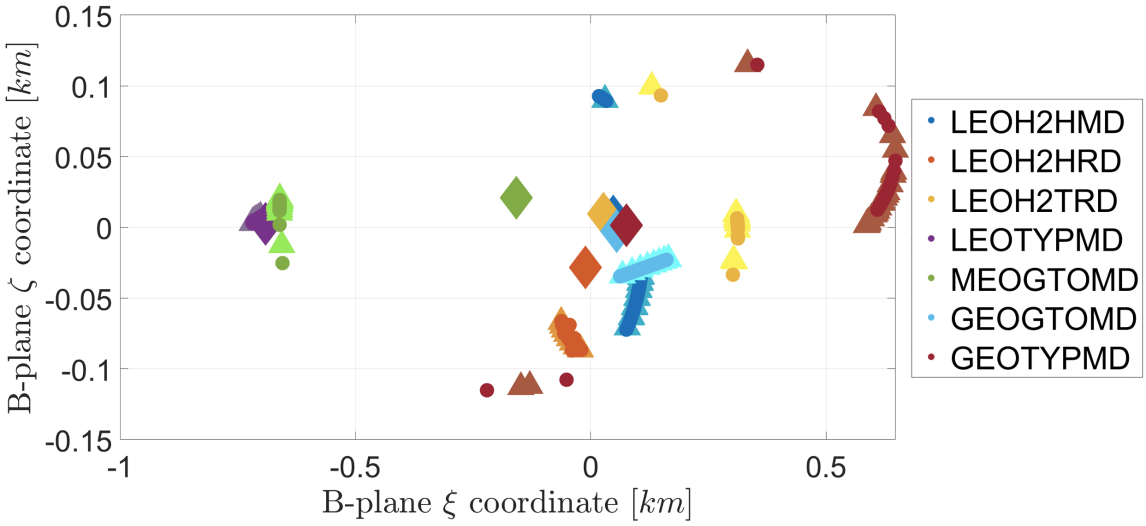


**Figure 13. Bplane position for the primary on ballistic (rhomboid), EO (dots), and FO (triangles) trajectories.**

When it comes to computational time in Fig 14, it encompasses $t_b$ computation, the guess-firing window selection, and the semianalytical iterative scheme. The envisioned procedure for tangential CAMs takes less than 0.1 s in almost every scenario without dependence on the starting point. The reason being, exploiting analytical propagators within the NLP formulation does not hinder efficiency.

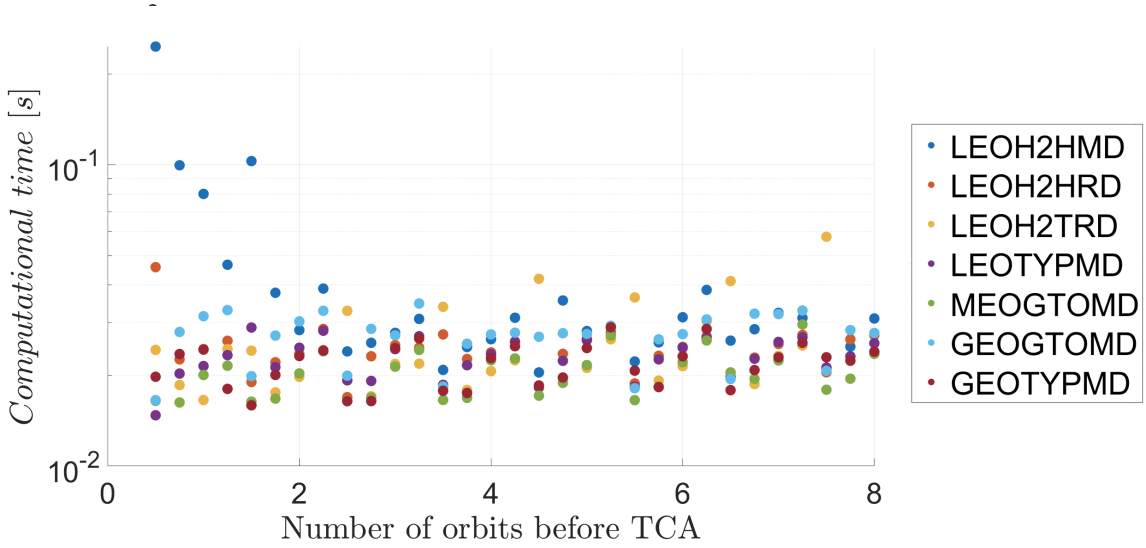


**Figure 14. Computational time for the FO CAM. The initial maneuvering points go from 0.5 to 8 before TCA.**

## CONCLUSIONS

This work intended to provide novel approaches for the design of a collision avoidance maneuver with tangential bang-bang control strategies. In this regard, a semi-analytical procedure for the solution of the Advanced Notification CAM problem has been presented, firstly by formulating the problem as a TPBVP, and then transforming it into an NLP problem. The analytical propagator developed by Bombardelli et al. in[12] has been exploited to drastically curb the computational time and attain a satisfactory PoC level. One could improve the model with intermediate evaluations of the analytical expression that describes the evolution of the generalized coordinates $(q_1, q_2, q_3)$ along a single thrusting arc. A useful add-on would be optimizing more firing widows all at once instead of constraining to a single one. Eventually, the pipeline could move the EO CAM showcased in[18] to a FO framework when facing three boundary value problems with return to the nominal orbit besides CAM design.

## REFERENCES


[1] M. F. Montaruli, L. Facchini, P. Di Lizia, M. Massari, G. Pupillo, G. Bianchi, and G. Naldi, "Adaptive track estimation on a radar array system for space surveillance," *Acta Astronautica*, Vol. 198, 06 2022, 10.1016/j.actaastro.2022.05.051.

[2] A. Cantoni, "Numerically Efficient Methods ForLow-Thrust Collision Avoidance Manoeuvres Design in GEO Regime," *73rd International Astronautical Congress (IAC),Paris, France, 18-22 September 2022*, 09 2022, pp. 1–12.

[3] C. Bombardelli and J. Hernando-Ayuso, "Optimal impulsive collision avoidance in low earth orbit," *Journal of Guidance, Control, and Dynamics*, Vol. 38, No. 2, 2015, pp. 217–225.

[4] C. Bombardelli, "Analytical formulation of impulsive collision avoidance dynamics," *Celestial Mechanics and Dynamical Astronomy*, Vol. 118, No. 2, 2014, pp. 99–114.

[5] J. A. Reiter and D. B. Spencer, "Solutions to rapid collision-avoidance maneuvers constrained by mission performance requirements," *Journal of Spacecraft and Rockets*, Vol. 55, No. 4, 2018, pp. 1040–1048.

[6] J. Hernando-Ayuso and C. Bombardelli, "Low-thrust collision avoidance in circular orbits," *Journal of Guidance, Control, and Dynamics*, Vol. 44, No. 5, 2021, pp. 983–995.

[7] A. De Vittori, M. Palermo, P. Di Lizia, and R. Armellin, "Low-Thrust Collision Avoidance Maneuver Optimization," *Journal of Guidance, Control, and Dynamics*, Vol. 45, 08 2022, pp. 1–15, 10.2514/1.G006630.

[8] R. Armellin, "Collision avoidance maneuver optimization with a multiple-impulse convex formulation," *Acta Astronautica*, Vol. 186, 2021, pp. 347–362.

[9] Z. Pavanello, L. Pirovano, and R. Armellin, "Long-Term Encounters Collision Avoidance Maneuver Optimization with a Convex Formulation," 01 2023.

[10] S. Dutta and A. Misra, "Comparison between convex and non-convex optimization methods for collision avoidance maneuvers by a spacecraft," *Acta Astronautica*, Vol. 202, 06 2022, 10.1016/j.actaastro.2022.06.020.

[11] S. Dutta and A. Misra, "Convex optimization of collision avoidance maneuvers in the presence of uncertainty," *Acta Astronautica*, Vol. 197, 05 2022, 10.1016/j.actaastro.2022.05.038.

[12] C. Bombardelli, G. Baù, and J. Peláez, "Asymptotic solution for the two-body problem with constant tangential thrust acceleration," *Celestial Mechanics and Dynamical Astronomy*, Vol. 110, No. 3, 2011, pp. 239–256.

[13] M. Maestrini, A. De Vittori, P. Di Lizia, and C. Colombo, "Dynamics-Based Uncertainty Propagation with Low-Thrust," 08 2022.

[14] M. Maestrini, A. De Vittori, J. L. Gonzalo, C. Colombo, P. Di Lizia, J. Arenas, M. Sanjurjo, A. Martín, P. Gago, and D. Antón, "ELECTROCAM: ASSESSING THE EFFECT OF LOW-THRUST UNCERTAINTIES ON ORBIT PROPAGATION," 01 2023.

[15] A. De Vittori, "Sensitivity analysis of collision avoidance manoeuvre with low thrust propulsion," 07 2023.

[16] C. Bombardelli, "Analytical formulation of impulsive collision avoidance dynamics," *Celestial Mechanics and Dynamical Astronomy*, Vol. 118, 11 2013, pp. 77–, 10.1007/s10569-013-9526-3.

[17] J. Peláez, J. M. Hedo, and P. R. d. Andrés, "A special perturbation method in orbital dynamics," *Celestial Mechanics and Dynamical Astronomy*, Vol. 97, No. 2, 2007, pp. 131–150.

[18] A. De Vittori, G. Dani, P. Di Lizia, and R. Armellin, "Low-Thrust Collision Avoidance Design for LEO Missions with Return to Nominal Orbit," 01 2023.